PHYSICAL REVIEW B VOLUME 22, NUMBER 6 15 SEPTEMBER 1980

Optical absorption edge of SiO_2

R. B. Laughlin
Bell Laboratories, Murray Hill, New Jersey 07974
(Received 25 April 1980)

The optical absorption spectrum of SiO_2 is calculated using tight-binding single-particle Hamiltonian and a screened Coulomb electron-hole interaction. The results of the calculation suggest strongly that all four features in ϵ_2 are excitonic resonances, that the gap in SiO_2 is 8.9 eV as indicated by internal photoemission, and that a Rydberg series of disallowed excitons exists beginning at 8.4 eV.

I. INTRODUCTION

Despite the technological importance of SiO_2 and the extensive experimental and theoretical work performed on it in recent years,[1,2] its optical absorption spectrum is still not completely understood. The reasons for this, which are numerous,[1] may be traced to the unfortunate confluence in this material of three factors antagonistic to simple analysis of optical spectra. The first is the large gap and small conduction-band effective mass SiO_2 has in common with alkali halides[3] and rare-gas solids.[4] This causes the electron-hole interaction to be large,[2-4] thus preventing computation of ϵ_2 using single-particle spectra[5-12] alone, but not sufficiently large to make the Frenkel picture of exciton formation quantitatively correct. The second is the structural complexity of SiO_2 in all its naturally occurring allotropes, particularly its glassy state. The third, and probably most important, is its lone-pair nature, i.e., its dense, overlapping, structure-dependent valence bands. These are sufficiently close together to be thoroughly mixed by the electron-hole interaction and therefore must be dealt with as a whole. The difficulty in interpreting the absorption spectrum of this material has had a number of serious consequences, the most significant being uncertainty[1,2] as to the size of its gap.

In this paper an attempt is made to shed some light on the nature of electronic excitations in SiO_2 via a model calculation of ϵ_2. The calculation is motivated by the observation[12] that matrix elements of the single-particle Green's function tend to be the same in *any* structure in which the integrity of the SiO_4 tetrahedron is preserved. An obvious corollary of this is that inclusion of the electron-hole interaction via a Green's-function technique[2] must also be insensitive to structure if the excitons are sufficiently small. That this is probably the case in SiO_2 is indicated by the remarkable similarity of the crystalline and amorphous absorption spectra. Insensitivity of the Green's function to structure has been used in this calculation as justification for adopting the highly symmetric but nonexistent β-cristobalite as a prototype structure and exploiting the favorable symmetry to make tractable the inclusion of a screened Coulomb electron-hole interaction. The calculation leads to sufficiently small excitons to justify to original approximations and suggests very strongly that

(1) all four features in ϵ_2 are excitonic resonances,

(2) the gap in SiO_2 is 8.9 eV, and

(3) there is a Rydberg series of disallowed excitons beginning at 8.4 eV.

II. EXPERIMENTAL SURVEY

Figure 1 shows reflectivity spectra of crystalline and amorphous SiO_2 (Refs. 13 and 14) taken by Philipp.[13] The gross features of the two, which are the same, include four peaks (10.3, 11.7, 14.0, and 17.3 eV), a rapid decrease in ϵ_2 below 10.3 eV, and a more gradual decrease above 18.0 eV. The evident insensitivity of ϵ_2 to disorder has led[15] to the speculation that its structure arises locally, possibly as a result of molecular symmetries preserved when the crystal is made glassy. The lowest two peaks are thought[2,15] to be excitons. Mott[15] has pointed out that the expected narrowing of the 10.3-eV peak at low temperatures does not occur, although some temperature dependence is observed.[16] The large width of this feature (~0.5 eV in α-quartz at room temperature) is thus perplexing and has led to the speculation[15] that phonon scattering is anomalously strong.

Reproduced in Fig. 2 are measurements by Appleton *et al.*[17] of optical density and photoconductivity in SiO_2 near the absorption edge. These show an "exponential edge" between 8.9 and 10.3 eV (probably present in the crystal as well) and a tail of absorption between 8.4 and 8.9 eV coinciding with a *quenching* of the photoconductivity. The residual absorption below 8.4 eV, found to vary

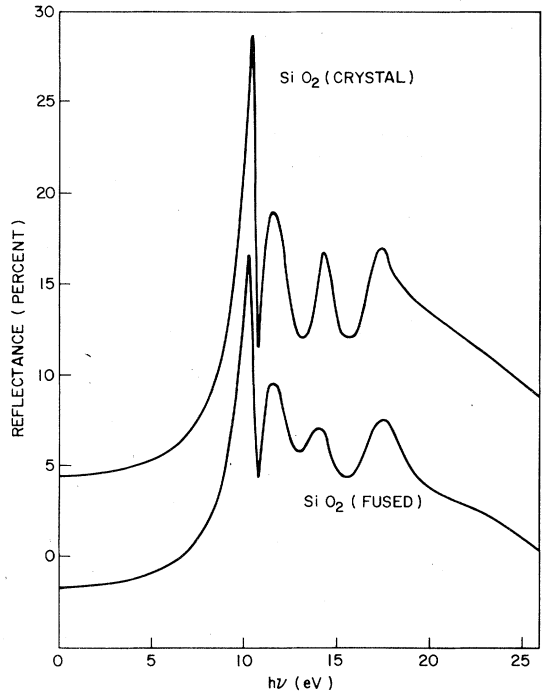

FIG. 1. Comparison of the reflectivities of crystalline and fused quartz taken from Ref. 13. The values for fused quartz have been lowered by 5%.

from one sample to another, was presumed to be due to impurities or defects. These authors explain the photoconductivity results by postulating a series of weakly allowed excitons broadened by random internal electric fields associated with disorder.[18] Below 8.4 eV, all absorption is due to impurity or defect ionization, which contributes

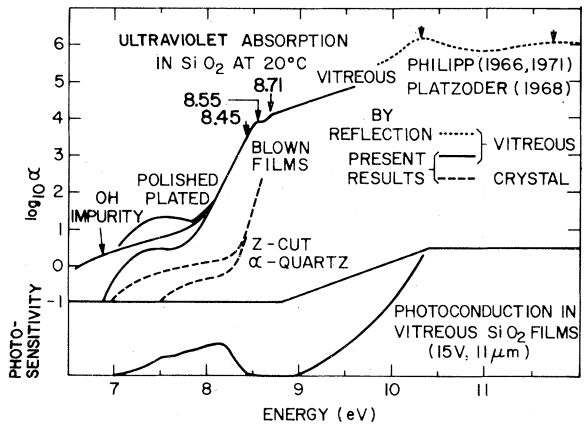

FIG. 2. Absorption coefficient and photoconductivity of SiO_2 taken from Ref. 17. Solid lines refer to the glass, dashed lines to the crystal. The dotted line is an estimate of α for amorphous silica based on reflectivity data from Ref. 13.

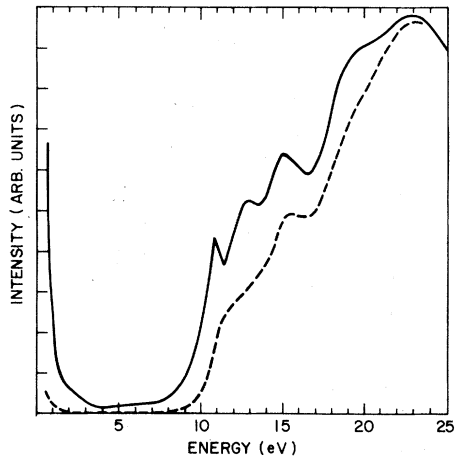

FIG. 3. Electron-energy-loss spectra of amorphous SiO_2 for $q=0$ (solid line) and $q=0.6$ Å^{-1} (dashed line) taken from Ref. 20.

free carriers and thus photoconductivity. Above 8.4 eV, excitonic absorption competes with defect absorption for the available light, and the photoconductivity drops. The resumption of photoconductivity at 8.9 eV corresponds either to the band gap (as would be the case in alkali halides) or to a threshold for ionizing excitons at electrodes or defects. Barely visible in Fig. 2 is some fine structure between 8.4 and 8.9 eV, suggestive of an excitonic Rydberg series. Recent attempts to reproduce this structure have not been successful.[19] Appleton *et al.* also measure the absorption coefficient of α-quartz between 7 and 9 eV and find the edge much more sensitive to temperature than that of amorphous silica. At 100°C they find a steep rise near 8.4 eV which moves to 8.7 eV as the temperature is lowered to −100°C.

Another experiment of potential significance in this problem is the electron-energy-loss result of Meixner *et al.*,[20] partially reproduced in Fig. 3. They report a loss spectrum at $\vec{q}=0$ in good agreement with $-\mathrm{Im}(1/\epsilon)$ as deduced from optical data. At $q=0.6$ Å^{-1}, however, all the features except that at 15 eV have washed out, and *no* disallowed exciton has become visible near 8.4 eV. There appears to be a slight upward shift of the peak at 15 eV as $\vec{q}$ is increased.

III. THE MODEL

In the presence of the electron-hole interaction ϵ_2 may be calculated by solving Dyson's equation

$$G = 1/(G_0^{-1} - V) \tag{1}$$

for the two-body Green's function G using the single-particle spectrum to generate G_0 and using a screened Coulomb interaction for V. Five major

approximations have been used in the present calculation.

Firstly, a simplified tight-binding Hamiltonian has been used to describe the single-particle excitations. The applicability of tight-binding Hamiltonians to this system and the significance of the parameters in them has been discussed in detail in Ref. 12. The valence states of SiO_2 may be seen from the pseudopotential charge densities[6] to be composed of oxygen $2p$ orbitals, bonding either with one another or with silicon orbitals. The O $2p$ orbitals perpendicular to the bond, which are forbidden by symmetry from interacting with silicon orbitals, broaden into a band centered at the O $2p$ energy referred to[13] as the "lone-pair-like" band. The O $2p$ orbitals along the bonds interact *strongly* with silicon orbitals to form the "bonding" band, roughly 5 eV lower in energy. The lone-pair-like band possesses[12] three peaks, each corresponding to one of three irreducible representations of the tetrahedral group: E, F_2 and F_1. The bonding band similarly possesses a peak at the high-energy edge which is F_2 like. The Hamiltonian used in the present calculation differs from that of Ref. 12 in that the silicon orbitals are not included explicitly and that the conduction states are represented by oxygen s orbitals alone.[21] The interaction between adjacent conduction orbitals is adjusted to reproduce the $0.3m_e$ effective mass obtained in the pseudopotential calculation,[6] and the orbitals are assigned an effective self-energy appropriate for producing a fundamental gap of 8.9 eV (Ref. 22). The parameters used in the single-particle Hamiltonian are listed in Table I.

Secondly, the β-cristobalite structure, which is that of silicon with oxygen atoms centered in the bonds, has been adopted. This is justified on the ground that neither the single-particle spectrum[12] nor ϵ_2 is very sensitive to structure, and it has the important effect of making the symmetry of the tetrahedron the symmetry of the problem. Figures 4 and 5 show the valence and conduction states of β-cristobalite calculated using the Hamiltonian of Table I. The x-ray photoemission spectra (XPS) of amorphous SiO_2 (Ref. 23) and the free-electron ($m^* = 0.3m_e$) (Ref. 6) densities of states are shown for comparison.

Thirdly, a dipole matrix has been adopted in which the electric field connects only oxygen sp orbitals on the same atom. This mechanism, which has been suggested before,[2] is physically reasonable and it tends to give the same result as more complicated mechanisms involving crossing transitions. The approximate equivalence of

TABLE I. Parameters used in the single-particle Hamiltonian. All energies are in eV. The notation for the interactions between O $2p$ orbitals is that of Ref. 12.

Holes	Electrons
$\epsilon^{O2p}_{bonding} = -6.98$	$\epsilon^{O2s} = 19.952$
$\epsilon^{O2p}_{nonbonding} = -1.739$	
$V_1^0 = -0.625$	$V = -1.842$
$V_2^0 = 0.0$	
$V_3^0 = -0.616$	
$V_4^0 = 0.108$	

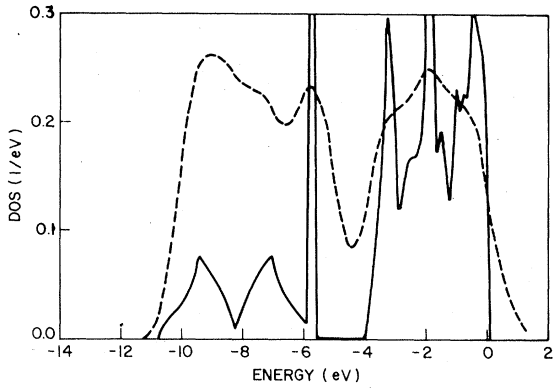

FIG. 4. Solid curve: Density of valence states of β-cristobalite calculated using the Hamiltonian of Table I. The normalization is the number of valence orbitals per unit cell. Dashed curve: Experimental x-ray photoemission spectroscopy of amorphous silica taken from Ref. 23.

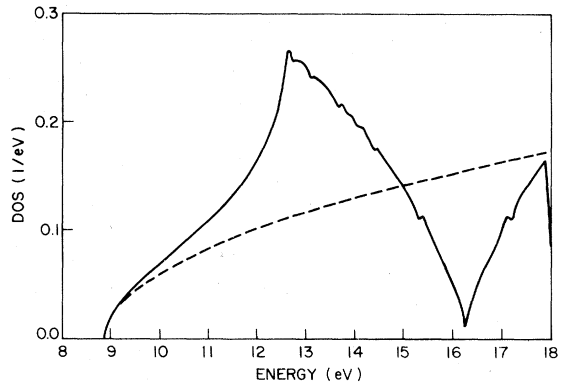

FIG. 5. Solid curve: Density of conduction states of β-cristobalite calculated using the Hamiltonian in Table I. The fine structure above 13 eV is computer noise. The normalization is the number of conduction orbitals per unit cell. Dashed curve: Free-electron density of states $(1/2\pi^2)(a^2m^*/\hbar^2)^{3/2}\sqrt{E}$, with $a = 5.26$ Å the β-cristobalite primitive translation length.

all mechanisms is a side effect of the small conduction-band mass. The conduction states most relevant to the absorption edge are those near the minimum at Γ.[6] As small m^* prevents states with large $\vec{K}$ from participating in the exciton wave function, the value of the conduction wave function in the vicinity of an atom is always well represented by its value on the atom.

Fourthly, the electron-hole interaction is assumed not to distort the tight-binding basis set and to take the value $e^2/\epsilon r$ between a pair of orbitals, where ϵ is the high-frequency dielectric constant of SiO_2 (2.38) and r is the separation of the orbital centers. If the valence and conduction orbitals are on the same atom, r is taken to be a bond length, the assumption being that most of the conduction wave function lies on the neighboring silicon atoms.[6] In addition, as the numerical solution of Eq. (1) requires a finite number of degrees of freedom, the electron-hole interaction is cut off beyond a separation of 8 Å. This distance corresponds to two effective Bohr radii and is selected for three reasons:

(1) Numerical considerations make this a convenient place to stop. The number of degrees of freedom grows as the cube of the cutoff radius.

(2) This is the distance at which the crystal and amorphous topologies begin to differ. (The first six-fold ring forms at 6 Å in β-cristobalite.)

(3) This is the point at which the $n=1$ exciton wave function and energy begin to stabilize. Most of the optical oscillator strength into parabolic excitons is into the $n=1$ state.

The most serious effect of the cutoff is to prevent the binding of excitons with primary quantum number $n=2$ and higher. It also induces a small upward shift in the $n=1$ binding energy, which may be taken into account using perturbation theory. The introduction of a cutoff is consistent with the notion that the features in ϵ_2 are local in origin.

Fifthly, a very limited, highly symmetric basis set is used to expand the two-body Green's function. Although the most natural position-space basis elements are those composed of a hole on atom j_h pointed in the αth direction and an electron on atom j_e, these are far too numerous for numerical work. They may be combined into two-body Bloch states having crystal momentum $\vec{q}$, the set of which forms a basis in which G is diagonal. For any $\vec{q}$, it suffices to know Green's-function matrix elements pertaining to a hole in the zeroth unit cell and an electron near that hole. These are given, in the absence of the electron-hole interaction, by

$$\langle j_h, j_e, \alpha | G_0(\vec{q}) | j_h', j_e', \alpha' \rangle = \sum_{\vec{k}} \sum_{n,m} \frac{\langle j_h, \alpha | \psi_h^n(\vec{k}) \rangle \langle j_e | \psi_e^m(\vec{k}+\vec{q}) \rangle \langle \psi_e^m(\vec{k}+\vec{q}) | j_e' \rangle \langle \psi_h^n(\vec{k}) | j_h', \alpha' \rangle}{E - E_e^m(\vec{k}+\vec{q}) + E_h^n(\vec{k}) + i\delta} , \tag{2}$$

where $|\psi_h^n(\vec{k})\rangle$ and $|\psi_e^m(\vec{k})\rangle$ denote the nth valence and mth conduction Bloch states at crystal momentum $\vec{k}$ having energies $E_h^n(\vec{k})$ and $E_e^m(\vec{k})$. As there are 12 valence orbitals in the unit cell, and 91 conduction orbitals within 8 Å of each of these, the number of relevant natural degrees of freedom is 1092. The size of this basis set is reduced in this calculation by drawing an analogy between this system and that in which the holes are infinitely heavy. In that case, the hole resides on only one oxygen atom at a time, each possible hole location producing a problem with the symmetry of the staggered form of ethane, i.e., D_{3d}. With only on-site dipole transitions allowed, no combinations of conduction orbitals except those in the completely symmetric A_{1g} representation need be considered. There are only 12 of these within 8 Å of the hole. Accordingly, in this calculation the basis has been restricted to elements combining a valence orbital in the zeroth cell with the lth ($l=1, 12$) A_{1g} shell of conduction orbitals about that valence orbital. This approximation corresponds physically to disregarding excitons of high angular momentum and is justified on the ground that these are not generally visible in optical spectra of wide-gap materials.[3,4] Further reduction is achieved at $q=0$ by exploiting tetrahedral symmetry. If the lth two-body basis element about $|j_h, \alpha\rangle$ is denoted by $|j_h, l(j_h), \alpha\rangle$, the action of an element T of the tetrahedral group is given by

$$T|j_h, l(j_h), \alpha\rangle = |T(j_h), l(T(j_h)), T(\alpha)\rangle . \tag{3}$$

Therefore, the two-body basis set may be transformed, without altering the form of the electron-hole interaction, which depends only on l, *into the irreducible representations of the holes*. As the model valence bands produce no Green's-function matrix elements between bonding and nonbonding O p orbitals, judicious choice of coordinates to remove degeneracy reduces the number of degrees of freedom within a representation to the number of shells (12).

IV. RESULTS

Consider first the case of model electrons in the presence of an infinitely massive hole. It suffices to solve Eq. (1) in the presence of a point charge on an oxygen atom, using as G_0 the single-particle Green's function generated from the conduction bands alone. The imaginary part of the Green's-function matrix element connecting the orbital at the center with itself is proportional to ϵ_2. Its value before and after the inclusion of the electron-hole interaction is shown in Fig. 6. In the presence of the interaction, two new features appear near the band edge: the ordinary parabolic exciton at 8.3 eV and an excitonic resonance, or hyperbolic exciton, near 10.5 eV. Both of these are well known[3,4,24] in the spectra of alkali halides and solid noble gases. The hyperbolic exciton is usually portrayed[3,4,24] as an electron-hole pair at the L point, bound in two dimensions and unbound in the third. (An excellent account of this in the case of CdTe has been given by Kane.[25]) Even though the L point and its singularity do not exist in α-quartz or amorphous silica, there are two reasons to suspect that this resonance should exist in these allotropes. Firstly, the size of the hyperbolic exciton in the two dimensions in which binding occurs is comparable[25] to that of the parabolic exciton. Thus, it should not be sensitive to long-range order, particularly the occurrence of sixfold rings of bonds which have been associated[12,26] with the peak at 13 eV. Secondly, the tendency of the electron-hole interaction to enhance ϵ_2 near the band edge is a well-known[27,28] phenomenon in the theory of Wannier excitons. In the presence of such a large electron-hole interaction, however, deviations of the tight-binding density of states from the effective mass value should cause the edge enhancement to become a peak. The oscillator strengths of the hyperbolic and parabolic excitons are comparable, the hyperbolic being about 1.6 times as strong. The calculated binding energy of the parabolic exciton is 0.58 eV, compared to a theoretical hydrogenic value of

$$E_b = (R_\infty/\epsilon^2)(m^*/m) = 0.72 \quad (4)$$

expressed in eV. This disparity disappears when the effect of the missing Coulomb tail is taken into account by perturbation theory, a somewhat surprising result in light of the small exciton size. The agreement is probably fortuitous since approximation errors are expected to be on the order of 10%. The parabolic exciton is roughly the size of the ideal hydrogenic exciton which has a radius of 4 Å. 83% of the state lies within 8 Å of the hole, compared with an ideal value of 76%. About 6% of the electron is on the hole, 24% is on nearest-neighbor oxygen atoms, 18% is on second neighbors, and 13% is on third neighbors. The hydrogenic radius lies between first and second neighbors.

Now consider the case of β-cristobalite. The band structures giving rise to Figs. 4 and 5 produce the joint density of states shown in Fig. 7. This is very similar to the one obtained from the pseudopotential band structure for α-quartz,[6] and indicates that, as in the pseudopotential results, structure in ϵ_2 arises *only* from matrix elements and the electron-hole interaction.

In Fig. 8 the contribution to ϵ_2 from transitions between the nonbonding (−5 to 0 eV in Fig. 4)

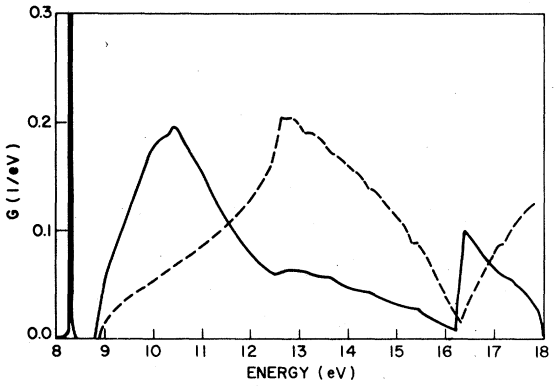

FIG. 6. Model ϵ_2 for the case of infinitely heavy holes with (solid line) and without (dashed line) the electron-hole interaction. The negative imaginary part of the Green's-function matrix element connecting the electron orbital at the center with itself is plotted. The real part of the Green's function has been computed as though the imaginary part were zero beyond 18 eV. This allows the effect of the electron-hole interaction to be checked with a sum rule, but makes the calculation inaccurate at high energy.

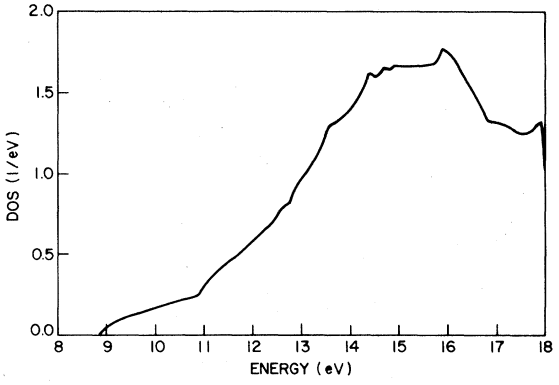

FIG. 7. Joint density of states for β-cristobalite. The normalization is the number of two-body orbitals per unit cell.

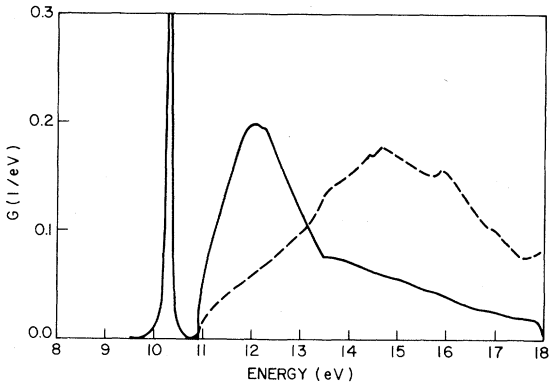

FIG. 8. Contribution to ϵ_2 of transitions from the nonbonding valence band into the conduction band with (solid line) and without (dashed line) the electron-hole interaction.

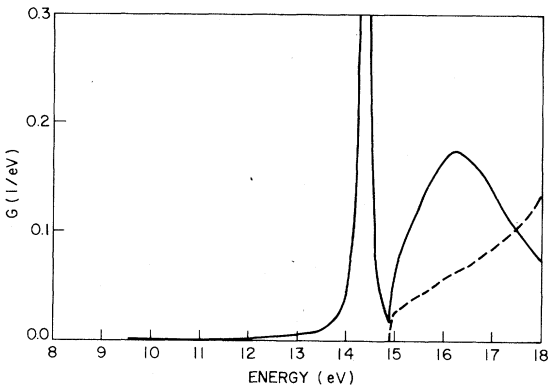

FIG. 9. Contribution to ϵ_2 of transitions from the bonding valence band into the conduction band with (solid line) and without (dashed line) the electron-hole interaction.

valence band and the conduction band with and without the electron-hole interaction is shown. The obvious similarity between this and Fig. 6 results from the tendency of the upper valence bands to behave as though they were composed of three heavy holes. The three structure-insensitive[12] peaks (0, −2, and −4 eV) in the nonbonding density of states are centered on the three energy eigenvalues at Γ of β-cristobalite. These give rise to six excitons, pairs of which to a good approximation lie in the irreducible representation of the tetrahedral group of the appropriate hole, i.e., F_1, F_2, or E. Thus, the F_1 and E excitons are dipole forbidden. Although departing from Γ breaks the selection rule quadratically in k (the single-particle Hamiltonian is even), the light-conduction-band mass assures that the $E^{5/2}$ (Ref. 29) absorption from the forbidden transitions is very weak. One important difference between Figs. 6 and 8 is the width of the parabolic exciton in the latter, attributable to the slightly dissipative nature of the F_2 part of the Green's function between 8.9 and 11 eV. This width corresponds physically to a lifetime for decay of the exciton (an A_1 electron bound to an F_2 hole) into a free A_1-F_1 electron-hole pair. The width of the peak is smaller in the model than it is in experiment, probably because of the excess symmetry in β-cristobalite.

In Fig. 9, the contribution to ϵ_2 from transitions from the bonding (−6 to −11 eV in Fig. 4) valence band into the conduction band with and without the electron-hole interaction is shown. The transitions giving rise to the unperturbed Green's function involve primarily the peak at −6 eV, which contains most[12] of the bonding F_2 character. The spectrum in Fig. 9 has been phenomenologically broadened to simulate decays of excitons into free electron-hole pairs involving a hole in the nonbonding band. The absence of such decays is a pathology of the model Hamiltonian stemming from the ability to decompose it exactly into bonding and nonbonding parts. The density of states is not sensitive to the value of the parameter (V_2^0) which mixes bonding and nonbonding states, and therefore no way exists to establish its value except by fitting the exciton width.

The quantity actually plotted in Figs. 8 and 9 is the imaginary part of a Green's-function matrix element associated with a normalized two-body degree of freedom consisting of a linear combination of four pairs of orbitals, an oxygen p, and an oxygen s on the same atom, on each of four atoms in the unit cell. The p orbitals point along the bonds in the bonding state, point normal to the bonds in the nonbonding state, and are combined to have F_2 symmetry in both cases. Accordingly, the coupling to the electric field is given by

$$\langle F_2^{\text{bonding}} | \vec{\mathrm{E}} \rangle = \sqrt{4/3}\, Ed\,, \tag{5}$$

$$\langle F_2^{\text{nonbonding}} | \vec{\mathrm{E}} \rangle = \sqrt{8/3}\, Ed\,, \tag{6}$$

with d the effective dipole matrix element between p and s orbitals on-site. Including a factor of 2 for spin degeneracy, one has for the electronic contribution to ϵ,

$$\epsilon_{\text{electrons}} = (-8\pi d^2/V)(\tfrac{8}{3} G^{\text{nonbonding}} + \tfrac{4}{3} G^{\text{bonding}})\,, \tag{7}$$

where V is the effective unit-cell volume as determined from the density of α-quartz. Assuming an experimental width for the 10.3-eV peak of 0.5 eV and a height of 7, and knowing the integral

$$\int_{10.3\text{-eV peak}} -\mathrm{Im}(G^{\text{nonbonding}})\, dE = 0.19\,, \tag{8}$$

one estimates a value for d of $1.2e$ Å, which is of the expected order. The relative strengths of the bonding and nonbonding contributions are at best

approximate, since the bonding state has silicon character[6] and thus relatively less strength on the oxygen atoms. However, it is clear that the assumption of on-site O $p \rightarrow$ O s transitions necessarily implies comparable contributions to ϵ from the bonding and nonbonding bands. The function ϵ_2 as given by Eq. (7), with arbitrary normalization, is compared with experiment in Fig. 10. The bonding contribution has been further broadened in Fig. 10 to agree better with experiment. With the band-gap fit to 8.9 eV, it is clear that a realistic electron-hole interaction reproduces the four peaks of the experiment at approximately the correct energies. The peaks near 10 and 12 eV originate in the lone-pair valence bands, while those at 14 and 16 eV start from the bonding states. The theory also yields correct relative strengths for all four peaks, indicating that in this energy range the oscillator-strength ratio given by Eqs. (5) and (6) is satisfactory. The displacements of the third and fourth peaks in the theory could be corrected by using heavier electrons, and it thus seems likely that the pseudopotential[6] m^* is slightly too small. As the binding mechanisms of the nonbonding and bonding excitons are similar, the separation of these energies must be that of the bonding and nonbonding F_2 peaks in the valence bands, seen in photoemission[23] to be 3.7 eV. Not readily visible in Fig. 10 but indicated by an arrow is a precipitous drop in the theoretical ϵ_2 at 8.9 eV corresponding to the band edge.

In Fig. 11, the on-site matrix element for the optically forbidden F_1 part of the Green's function with and without the electron-hole interaction is shown. The F_1 analog of the visible excitonic

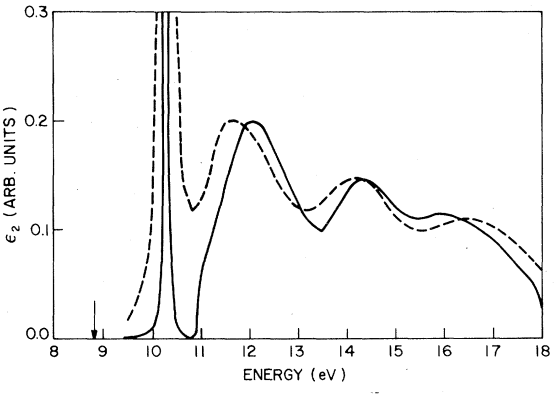

FIG. 10. Superposition of the solid curves in Figs. 8 and 9 (solid curve) compared with the experimental ϵ_2 (dashed curve) for amorphous SiO_2 taken from Ref. 14. The nonbonding contribution has been convolved with a Gaussian of 1-eV width. The heights of the peaks at 12 eV have been equated. The arrow locates the band edge, where a precipitous drop to zero of the theoretical ϵ_2 occurs.

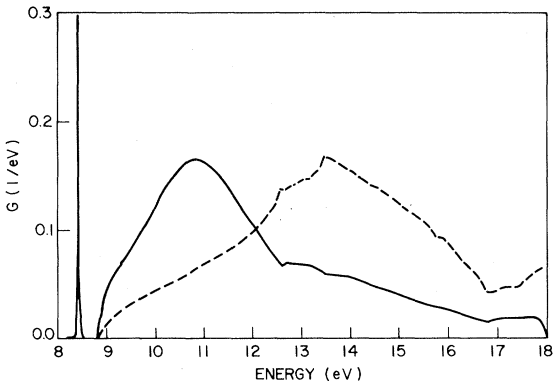

FIG. 11. Imaginary part of the Green's-function matrix element between the on-site ($l=1$) F_1 state and itself with (solid line) and without (dashed line) the electron-hole interaction.

resonance at 10.3 eV is thus a disallowed exciton at 8.4 eV. This is only the first in a Rydberg series, visible in this plot by virtue of its large amplitude for finding the electron and hole on the same atom. The disallowed nature of these excitons arises from a cooperative effect between transitions on all four atoms in the tetrahedron, and thus ought to be violated in $\epsilon(\vec{q})$ for fairly small $\vec{q}$. Along symmetry directions, however, where the computation of $\epsilon(\vec{q})$ is still simple, it is evident that the disallowed excitons *contribute only to the transverse part of* ϵ. For example, constraining $\vec{q}$ to lie between Γ and X reduces the symmetry only to C_{2v}, with the longitudinal part of ϵ comprising an A_1 representation. The set of nonbonding O $2p$ orbitals contains two A_1 representations: the vector (F_2) state pointing along $\vec{q}$ and the E state formed by negating two orbitals in the F_2 state. The E part of the Green's function, which thus mixes with the F_2 part in $\epsilon_{\|}$ as $\vec{q} \rightarrow X$, is virtually identical to the F_1 part at Γ, except that it lies 4 eV higher. Therefore, as $\vec{q} \rightarrow X$, a disallowed E excitonic resonance near 12.3 eV should become visible in $\epsilon_{\|}$, but the F_1 exciton should not. Similarly, constraining $\vec{q}$ to lie between Γ and L reduces the symmetry only to C_{3v}, with the A_1 representation again the relevant one. In this case, however, the only A_1 representation is the F_2 state pointing along $\vec{q}$, and thus the dimensionality of the problem is still 12, and neither the E nor the F_1 exciton is visible. Plotted in Fig. 12 is the theoretical value for the contribution to $\epsilon_1(\vec{q})$ at $\vec{q}=L$ (~ 0.7 Å^{-1}) produced by transitions from the nonbonding valence band. The only significant difference between this ϵ_2 and that of Fig. 8 is a slight tendency for the unperturbed Green's function to tail near 10.5 eV, and thus cause the gap in $\epsilon_{\|}$ to fill up. This effect is due to the failure of the valence bands to function as three distinct

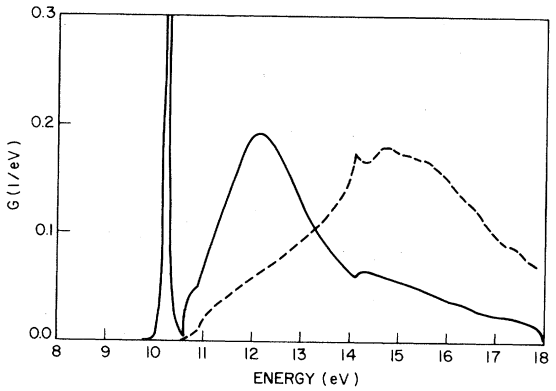

FIG. 12. Contribution to the longitudinal part of $\epsilon_2(\vec{q})$ at $\vec{q}=L$ from transitions from the nonbonding valence band with (solid line) and without (dashed line) the electron-hole interaction.

holes at $q \neq 0$ and is probably more severe in α-quartz and the glass than in this model.

V. DISCUSSION

As it is based on an unparametrized electron-hole interaction, the good agreement between theory and experiment in Fig. 10 is persuasive evidence that the gap in SiO_2 is near 8.9 eV indicated by photoconductivity.[17,22] It also indicates that the dipole-forbidden excitons between 8.4 and 8.9 eV suggested by Appleton *et al.*[17] exist. Forbidden excitons with nonzero angular momentum should,[28] in principle, contribute to the optical density near the band edge, and thus a careful measurement of the edge of α-quartz at low temperature might be in order. It should be pointed out, however, that if the gap in α-quartz is indirect, direct excitons might be lifetime broadened via phonon-assisted decay.[30]

There are a number of reasons why the forbidden excitonic absorption in the glass might be a continuum. Dow-Redfield–type tailing[18] might be important, as might inhomogeneous broadening due to fluctuations in the exciton binding energy or allowed oscillator strength produced by weakening of the $\vec{k}=0$ selection rule due to disorder. One piece of evidence supporting the latter explanation is the large temperature dependence of the edge in α-quartz compared to that in the glass.[17] An increase in band gap with increasing temperature should appear in both spectra, whereas breaking of the momentum selection rule would occur only in the crystal. One would predict from such a picture that the absorption edge of the glass would be similar to that of the liquid at the glass transition temperature.

It seems likely that the width of the 10.3-eV resonance, given incorrectly by the model, is attributable in part to the Si–O–Si bend angle in SiO_2. Dissipation in the F_2 Green's function is related to the loss of tetrahedral symmetry at $k \neq 0$, and should thus be more prevalent when tetrahedral point symmetry does not exist at all.

In this model the four peaks in ϵ_2 between 8 and 18 eV are analogs of features seen in alkali halides and rare-gas solids. As in these other wide-gap materials,[3,4,24] the holes behave as though they are distinct and heavy, and the only relevant conduction band is the lowest one. The formation of the two lower peaks (and thus of the two higher ones) differs qualitatively in this model from the picture suggested by Pantelides[2] in that neither is associated directly with a peak in the single-particle ϵ_2. This is especially important in light of the possibility[31] that the peak at 11 eV in the pseudopotential ϵ_2 (Ref. 6) is not correct. The grid in that calculation consisted only of 13 points in the α-quartz irreducible Brillouin zone and was used to construct a histogram of width $\Delta E = 0.5$ eV which was later smoothed. The step giving rise to the peak at 11 eV is quite small and could conceivably be noise.

The failure of the disallowed excitons to be visible in $\epsilon_2(q)$ for $\vec{q} \neq 0$ has been shown to be expected along symmetry directions, but not in general. A more universal argument may be applied if $\vec{q}$ is small. Since $\vec{q}$ is responsible for the destruction of tetrahedral symmetry, the amount of F_2 character in the disallowed exciton may be expanded in a power series in $\vec{q}$. Since this exciton is a pseudovector, however, it can be converted to a vector only via cross product with $\vec{q}$. This forces the exciton dipole moment to be transverse to lowest order in $\vec{q}$, and thus invisible in energy-loss spectroscopy.

The peak at 15 eV in Fig. 3 is the last to wash out with increasing $\vec{q}$. A possible explanation for this is that the bonding valence bands involve only two irreducible representations and are wider than the nonbonding bands. In β-cristobalite there are four bonding bands, two of which are relatively flat and generate the peak in the density of states at −6 eV. These two are completely F_2 in character and *transverse*. The two remaining bands form the peaks at −7 and −9 eV and share the A_1 and longitudinal F_2 character, the latter being concentrated near −6 eV. The longitudinal F_2 character in the two-body Green's function therefore comes primarily from one band and is not strongly smeared until $\vec{q}$ approaches X. One consequence of this picture is that the parabolic exci-

ton (15 eV) should track the downward dispersion of the longitudinal F_2 valence band between −6 and −8 eV, and thus disperse upward by about 1 eV by $q = 0.6$ Å^{-1}. This is consistent with the trend observed in Fig. 3.

ACKNOWLEDGMENTS

I would like to thank M. Schlüter, P. Platzman, E. O. Kane, J. D. Joannopoulos, and D. J. Chadi for helpful discussions.

[1]See D. L. Griscom, J. Non-Cryst. Solids 24, 155 (1977).
[2]S. T. Pantelides, in *The Physics of SiO_2 and its Interfaces*, edited by S. T. Pantelides (Pergamon, New York, 1978), p. 80.
[3]J. C. Phillips, Phys. Rev. 136, A1705 (1964).
[4]J. C. Phillips, Phys. Rev. 136, A1714 (1964).
[5]S. T. Pantelides and W. A. Harrison, Phys. Rev. B 13, 2667 (1976).
[6]J. R. Chelikowsky and M. Schlüter, Phys. Rev. B 15, 4020 (1977); M. Schlüter and J. R. Chelikowsky, Solid State Commun. 21, 381 (1977).
[7]K. L. Yip and W. B. Fowler, Phys. Rev. B 10, 1400 (1974).
[8]P. M. Schneider and W. B. Fowler, Phys. Rev. Lett. 36, 425 (1976).
[9]E. Calabrese and W. B. Fowler, Phys. Rev. B 18, 2888 (1978).
[10]S. Ciraci and I. P. Batra, Phys. Rev. B 15, 4923 (1977).
[11]F. Yndurain, Solid State Commun. 27, 75 (1978).
[12]R. B. Laughlin, J. D. Joannopoulos, and D. J. Chadi, Phys. Rev. B 20, 5228 (1979).
[13]H. R. Philipp, Solid State Commun. 4, 73 (1966); J. Non-Cryst. Solids 8–10, 627 (1972).
[14]G. Klein and H. U. Chun, Phys. Status Solidi B 49, 167 (1972).
[15]N. F. Mott, Adv. Phys. 26, 363 (1977).
[16]K. Platzöder, Phys. Status Solidi 29, K63 (1968).
[17]A. Appleton, T. Chiranjivi, and M. Jafaripour-Ghazvini, in Ref. 2, p. 94; see also Z. A. Weinberg, G. W. Rubloff, and E. Bassous, Phys. Rev. B 19, 3107 (1979).
[18]J. D. Dow and D. Redfield, Phys. Rev. B 5, 594 (1972).
[19]D. Griscom, private communication.
[20]A. E. Meixner, P. M. Platzman, and M. Schlüter, in Ref. 2, p. 85.
[21]W. B. Fowler, P. M. Schneider, and E. Calabrese, in Ref. 2, p. 70.
[22]T. H. DiStefano and D. E. Eastman, Solid State Commun. 99, 2259 (1971).
[23]B. Fischer, R. A. Pollak, T. H. DiStefano, and W. D. Grobman, Phys. Rev. B 15, 3193 (1977).
[24]J. C. Phillips, *Fundamental Optical Spectra of Solids*, Solid State Physics (Academic, New York, 1966), Vol. 18.
[25]E. O. Kane, Phys. Rev. 180, 852 (1969).
[26]M. Thorpe, in Ref. 2, p. 116.
[27]R. S. Knox, *Theory of Excitons*, Solid State Physics, Suppl. 5 (Academic, New York, 1963).
[28]R. J. Elliott, Phys. Rev. 108, 1384 (1957).
[29]First-order breakdown of the selection rule leads to $E^{3/2}$ dependence. (See Ref. 28.)
[30]A discussion of Polaronic effects in exciton formation may be found in E. O. Kane, Phys. Rev. B 18, 6849 (1978).
[31]M. Schlüter, private communication.